红外与激光工程
INFRARED AND LASER ENGINEERING
EI, SCOPUS, CSCD等收录期刊

超精密位移台计量特性的差动式平面镜干涉溯源分析

闫勇刚 吴正兴 李直 汤宇祺

Traceable analysis of the performance of an ultra-fine positioning stage using a differential plane mirror interferometer

Yan Yonggang, Wu Zhengxing, Li Zhi, Tang Yuqi

在线阅读 View online: https://doi.org/10.3788/IRLA20210070

您可能感兴趣的其他文章

Articles you may be interested in

超细镁铝尖晶石凝胶注模用浆料的制备

Preparation of ultra-fine magnesium aluminate spinel slurry for gelcasting forming

红外与激光工程. 2018, 47(11): 1121004-1121004(7) https://doi.org/10.3788/IRLA201847.1121004

基于激光干涉法测水介质正弦压力的动态校准技术

Dynamic calibration technology for measuring sinusoidal pressure of water medium based on laser interferometry

红外与激光工程. 2019, 48(8): 805003-0805003(7) https://doi.org/10.3788/IRLA201948.0805003

多维栅格标准样板的制备与表征

Development and characterization of multi-dimension grid standard template

红外与激光工程. 2019, 48(5): 503006-0503006(7) https://doi.org/10.3788/IRLA201948.0503006

3D激光扫描共聚焦显微镜计量特性分析及测试

Measurement characteristics analysis and test of 3D laser scanning confocal microscope

红外与激光工程. 2018, 47(8): 817005-0817005(8) https://doi.org/10.3788/IRLA201847.0817005

4m SiC主镜硬点定位机构指标性能分析

Performance analysis of hardpoint positioning mechanism for 4 m SiC primary mirror

红外与激光工程. 2019, 48(4): 418004-0418004(5) https://doi.org/10.3788/IRLA201948.0418004

激光锁定Fabry-Perot干涉仪精密测量电容

Precise capacitance measurement by laser locking Fabry-Perot interferometer

红外与激光工程. 2019, 48(5): 517001-0517001(9) https://doi.org/10.3788/IRLA201948.0517001

Traceable analysis of the performance of an ultra-fine positioning stage using a differential plane mirror interferometer

Yan Yonggang[1,2], Wu Zhengxing[1], Li Zhi[2], Tang Yuqi[2]

(1. School of Mechanical & Power Engineering, Henan Polytechnic University, Jiaozuo 454003, China;
2. Physikalisch-Technische Bundesanstalt (PTB), Braunschweig D-38116, Germany)

Abstract: Ultra-fine positioning stages are the indispensable components in many areas of nanotechnology and advanced material analysis, and are always integrated into analytical devices such as Scanning Probe Microscope (SPM), optical microscope. The mechanical properties of the microscopic measurement system were strongly influenced by the nano-mechanical performance of an ultra-fine positioning stage. A traceable calibration setup for investigating the quasi-static performance of nano-positioning stage was developed, which utilized a differential plane mirror interferometer with double-pass configuration from the National Physical Laboratory (NPL). Based on an NPL-developed FPGA and LabView, the laser interferometric data acquisition (DAQ) and data decoding system with high precision and stable frequency was built up to enable traceable quasi-static calibration of ultra-fine nano positioning stages. Furtherly, the proposed system was used to calibrate and analyze the metrological characteristics of nano-positioning stages. The experimental results have proven that the calibration setup can achieve a noise floor lower than 10 pm/$\sqrt{\text{Hz}}$ under nearly open-air conditions. The calibrated pico-positioning stage has an excellent nano-mechanical performances, such as the linearity of being lower than 1.2×10^{-6}, the resolution of being up to 40 picometer, good repeatability and stabilization. The results indicate that the proposed method and system can be used to measure the performances of the ultra-fine positioning stages, and furtherly be used for pico-indentation with indentation depths down to a few picometers and the large-scope measurement at the atomic scale.

Key words: nanometrology; laser interferometry; ultra-fine positioning stages; traceability

CLC number: TH744 **Document code:** A **DOI:** 10.3788/IRLA20210070

超精密位移台计量特性的差动式平面镜干涉溯源分析

闫勇刚[1,2], 吴正兴[1], 李　直[2], 汤宇祺[2]

(1. 河南理工大学 机械与动力工程学院，河南 焦作 454003;
2. 德国联邦物理技术研究院，德国 布伦瑞克 D-38116)

摘　要：超精密纳米位移台常用于扫描探针显微镜、光学显微镜等高精度分析仪器中,其纳米机械性能的精密计量和校准对显微测量系统的性能起着关键作用。基于一种双通道结构差动式平面镜干涉测量与校准方法 (英国国家物理实验室),文中对一种超精密位移台的关键计量特性进行了定量研究。构建了基于现场可编程门阵列 (FPGA) 和 LabView 的高精度稳频激光干涉数据采集和数据解码系统,

收稿日期:2021−01−27; **修订日期:**2021−04−08

基金项目:国家自然科学基金面上项目 (51775174);河南省重点科技攻关计划项目 (212102210323);河南省高校基本科研业务费专项资金 (NSFRF180332)

作者简介:闫勇刚,男,副教授,硕士生导师,博士,主要从事光学精密测量、视觉测量等方面的研究。

使其可溯源超精密纳米位移台的准静态校准计量特性。进一步地,利用该干涉测量系统对超精密位移台的计量特性进行了校准和分析。测试结果显示,该激光干涉校准系统在准开放环境中的背景噪声低于 10 pm/$\sqrt{\text{Hz}}$;该超精密位移台具有优良的纳米机械性能,其线性度低于 1.2×10^{-4},分辨率达 40 pm,重复性和稳定性较好。上述对校准设备准静态性能和对纳米位移台计量特性的测试结果表明,所提出的方法和系统能够对纳米位移台进行计量,从而用于小于几皮米的皮米级压痕测量以及原子尺度上的大范围测量。

关键词:纳米计量; 激光干涉; 超精密定位台; 溯源

0 Introduction

Developments in precision manufacturing, piezo-electric material processing, position-sensing and control system, have increased the demand for ultrahigh precision micro- and nano-positioning stages with pico-meter displacement resolution. Such stages are the indispensable components of industrial and metrological instruments, precision measurement, nano-technology, and advanced material analysis[1−4], and are always integrated into analytical devices such as SPM, optical microscope, scanning interferometer and manufacturing devices because of their high resolution, excellent linearity, high positioning accuracy and repeatability, and so on.

Commercial SPMs are able to determine the thickness of a single or few layer two-dimensional materials with an accuracy of better than 0.1 nm[5]. Research-aimed atomic force microscopy (AFM) is ready for experimental investigations of the nano-electromechanical interaction between AFM probes and the sample under test at the atomic scale[6]. For a pico-indentation instrument aiming to produce full plastic deformation at the atomic scale with a super-sharp ultra-nanocrystalline diamond tip, an ultra-precision positioning stage with a resolution down to sub-10 pm is one of the essential components[7].

Recent applications in nanotechnology require that not only the nanopositioning of the commercial stages have to be based on precise measurements but the traceability of the measuring technique has to be ensured up to the primary standard. Traceable measurements of the nanopositioning stages are classified as both main configurations of laser interferometers: homodyne and heterodyne. The former setup uses a single frequency laser source and exhibits high measurement accuracy. The latter is of larger nonlinearity because of the errors caused by frequency and polarization mixing[8−9], and its configuration is more complicated than the homodyne. While the displacements of nanopositioning stages are large multiples of the wavelength, the interferometer can offer virtually unlimited dynamic range within the coherence length of the laser source. However, it is a great challenge for the positioning far below the wavelength using the traditional optical coherent interferometry.

In this work, a reliable calibration method and system for traceable performance evaluation of ultra-fine stage is realized using a differential plane mirror interferometer from NPL, the magnitude of the cyclic error of which is ±20 pm[10]. Compared with the nanometrology technology, such as double-frequency laser interferometer, beat frequency Fabry-Perot interference[11−12] and X-ray interferometer[13], the proposed method and system are easier to control and implement, and also is of high accuracy and good stabilization.

1 Proposed method and system configuration

A reliable calibration method for the investigation of the quasi-static performances for nano-positioning stage is proposed and the corresponding system is developed, which consists of an optical system based on a differential plane mirror interferometer with double-pass configuration from NPL[14], an NPL-developed FPGA-based interferometric data acquisition and decoding system, and mechanical system.

By means of the different plane mirror interfer-

ometer, the movement displacement of the ultra-fine positioning stage can be transmitted to the phases of the photoelectric signals. The variation of the signals is acquired by the data acquisition and decoding system, and the displacement is calculated successfully. On the base, the method and its system can be used to calibrate and trace the metrological characteristics of nano-positioning stages effectively and creatively.

1.1 Optical system

The optical configuration of the NPL Jamin Differential Plane Mirror interferometer is shown as Fig.1. The interferometer based on a common-path optical configuration is regarded as a standard. The laser beam (λ=632.991 nm) coming from a frequency-stabilized He-Ne laser (Thorlabs, intensity stabilization of ±0.2%) is firstly coupled into a polarization-maintaining single-mode (PM) fiber through Faraday optical isolator and aperture, and then delivered to the integrated interferometric calibration system, thereby separating the heat generated by the laser from the experimental devices. This optical fiber delivery system has also effectively decoupled the laser source from the calibration setup, and therefore offered flexibility for the following calibration work.

The decoupled laser beam enters the Jamin interferometer after it is collimated by an aspheric lens, and forms the linearly reference and measurement laser beams. Then they are reflected back from the U-shaped reference and measurement mirror respectively to produce an interference pattern incident.

Owing to the phase quadrature coatings at the corresponding positions on the Jamin beamsplitter, two phase-quadrature interference signals (sin and cos, in Fig.1) are generated and captured by the photo detectors, given as the optimum signal-to-noise conditions for fringe counting and subdividing.

While the moving measurement mirror travels attached to an ultra-fine stage which is driven by a piezoelectric actuator, its relative displacement can be expressed in Eq.(1):

$$L = N \cdot \frac{\lambda}{4} \tag{1}$$

where N is the number of the interferometric fringe, and λ is the wavelength of the frequency-stabilized He-Ne laser beam.

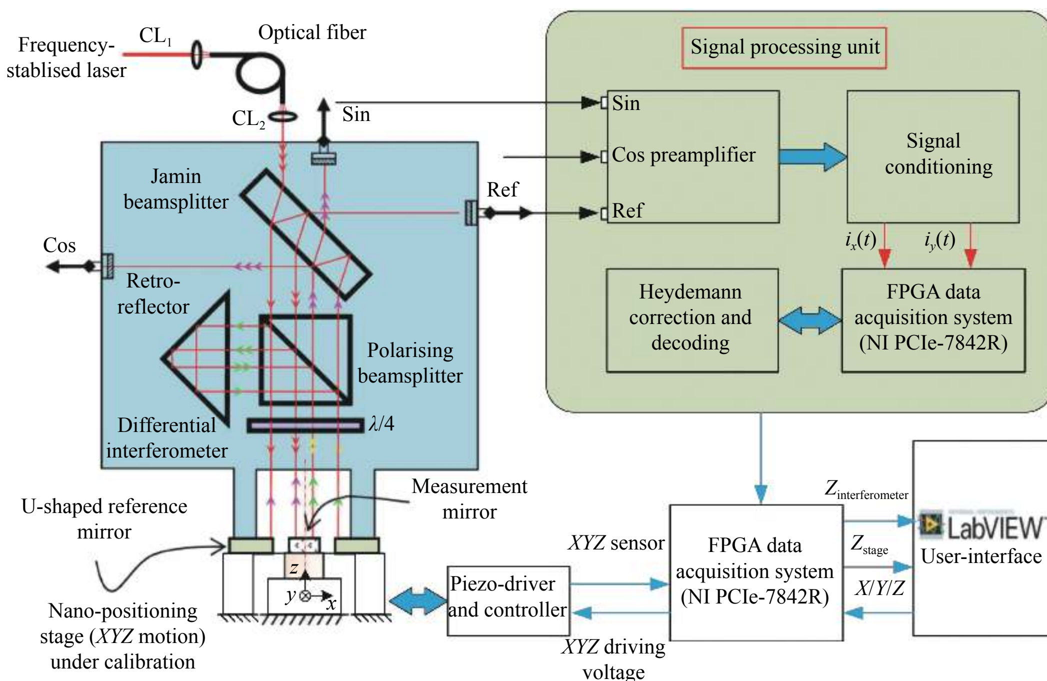

Fig.1 Traceable calibration layout for quality control of micro-/nano-positioining stages

1.2 Mechanical system

A mechanical system of the calibration setup has been fabricated correctly to be in accordance with the design and configuration of the NPL interferometer. The interferometer block together with its U-shaped reference mirror is supported by three evenly-distributed columns made of invar. Two micrometers located on the V-groove of the invar columns (not shown in Fig.1) are used to align the measurement beams with the measurement mirror, which is fixed onto the stage under calibration. Three additional micrometers are utilized for fine adjustment of the U-shaped reference mirror. Care has been taken to make sure that (1) the reference mirror is vertical to the reference beams, (2) the optical path difference between the reference and the measurement beams is close to zero, and (3) the calibrated setup should be let stand still for 72 h after the adjustment and tight fixation.

1.3 Data acquisition and signal processing

The phase quadrature interference signals (sin and cos, shown in Fig.1) together with the reference signal are firstly transmitted into a NPL-developed preamplifier for current-to-voltage conversion, amplification and denoising. The signals are then processed using a NPL-developed signal optimizing unit to remove the direct current (DC) offset of the signals, compensate for the potential laser intensity fluctuation, and amplify the analog signals in such a way that they can match with the full dynamic range of the analog to digital converters (ADCs) on the field-programmable gate array (FPGA) card. The magnified quadrature interference signals $i_x(t)$ and $i_y(t)$, acquired from the signal conditioning unit have nearly zero-offset, and a magnitude of about ±9 V. And they are converted into a displacement through fringe counting and subdividing.

The two signals $i_x(t)$ and $i_y(t)$ can be expressed in Eq.(2):

$$\begin{cases} i_x(t) = i_{x0} + C_x \cos\varphi(t) \\ i_y(t) = i_{y0} + C_y \sin[\varphi(t) + \varphi_0] \end{cases} \tag{2}$$

where i_{x0} and i_{y0} are the DC offsets; C_x and C_y are the different AC amplitudes for the signal, and φ_0 is the phase-quadrature error between the two signals.

In the case of zero-path difference, the displacement ΔL of the measurement mirror is proportional to the phase shift $\Delta\varphi$ in interference signals during the period of $[t_0, t_1]$, which can be expressed in Equation (5):

$$\Delta L = \frac{\Delta\varphi}{8\pi} \times \lambda = \frac{\varphi(t_1) - \varphi(t_0)}{8\pi}\lambda \tag{3}$$

where λ is the laser wavelength.

Subsequently, a FPGA-based DAQ system (NI PCIe-7842R) is used to acquire the optimized interference signals $i_x(t)$ and $i_y(t)$. This multifunction reconfigurable DAQ system features a sampling rate of 200 kS/s with a user programmable FPGA for high-performance onboard signal processing and direct control over I/O signals. This DAQ system is also capable of A/D conversion per channel (16 bit single-ended) for independent timing and triggering. It is therefore especially suitable for high-speed acquisition of phase-quadrature interference signals without introduction of additional phase shifts or retardation between the two signals $i_x(t)$ and $i_y(t)$.

The digitized interference signals read by this DAQ system are firstly normalized using the Heydemann correction to compensate for the five parameters such as offsets, gains, and signal phase $[i_{x0}, i_{y0}, C_x, C_y, \varphi]$[15], those tend to be time-varying. Thus, the nonlinear error within this homodyne interferometer will be eliminated as much as possible. This nonlinearity correction and thereafter interferometric decoding is realized by a NPL-developed LabView® program. The DAQ system is also used to provide the analog signals for the controller of nano positioning stages and acquire their displacement sensor signals by a user LabView interface software.

1.4 Quasi-static performance test results of the calibration setup

The interferometric calibration setup is mounted on an optical vibration isolation platform, and works under nearly open-air conditions, as shown in Fig.2. More care is taken that a plastic cover is used to isolate the heat generated by the laser from the experimental devices or

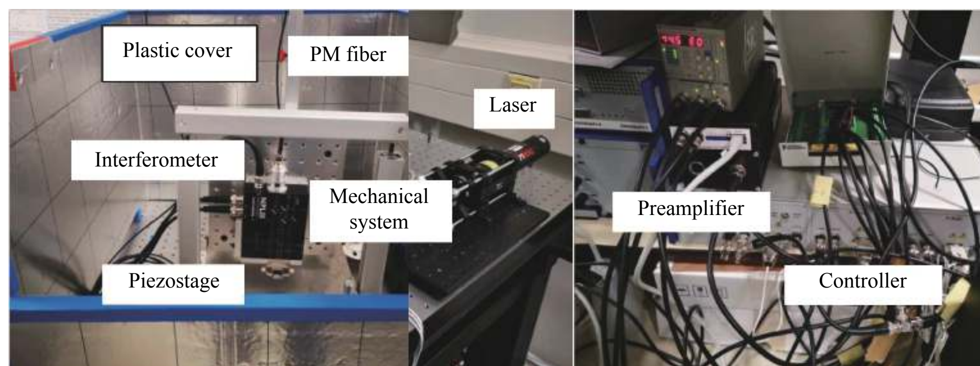

Fig.2 Interferometric calibration setup

other heat source so as to eliminate the influence to the calibrated ultra-fine stage.

Figrue 3(a) shows the mid-term stability and drift of the interferometer within 50 s, which is a typical duration for one nanoindentation process including loading, holding and unloading procedures, respectively.

The corresponding noise spectrum density, obtained by using short-time Fourier transform with Hanning window, is illustrated in Fig.3(b). The vertical and horizontal coordinates in this figure are of logarithmic forms. It can be seen from Fig.3 that the calibration setup has a drift smaller than 200 pm within the period of 50 s, and a noise floor lower than 10 pm/$\sqrt{\text{Hz}}$. So, the system

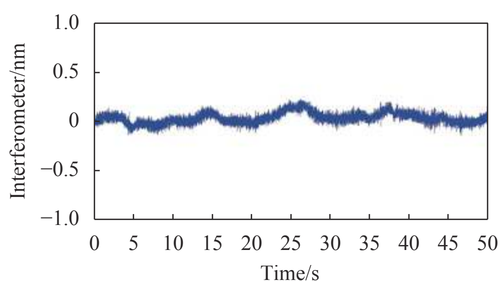

(a) Stability of the calibration setup

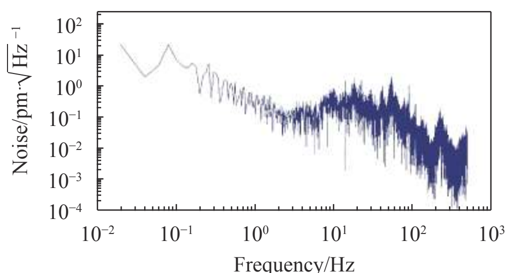

(b) Noise spectrum of the interferometer

Fig.3 Experimental investigation of the quasi-static performance of the interferometric calibration setup

measurement accuracy and stabilization can meet the requirement during calibration.

To evaluate the relative position and orientation between the optical axis of the interferometer and the measurement mirror mounted onto the z axis of the piezostage within the z-axis motion range, an experiment was carried out under nearly open-air conditions. The z-axis motion deviations of the interferometric calibration setup are measured, and a polynomial fitting is done using least square estimation, as shown in Fig.4.

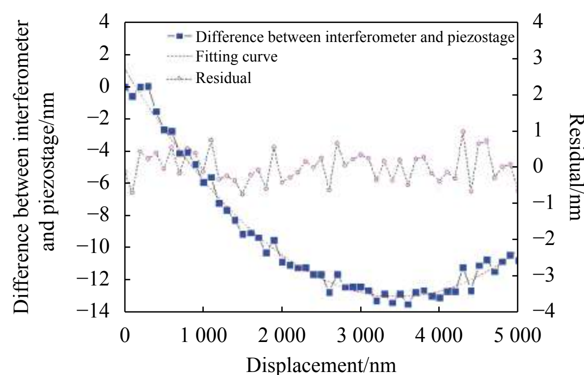

Fig.4 Experimental investigation of the z-axis motion performance of the interferometric calibration setup

Seen from Fig.4, the interferometric measurement errors are of non-linear with the displacement over the range, and obviously there exists angular variation between the optical axis of the interferometer and the measurement mirror due to possible temperature fluctuation. They may be also caused by other reasons such as the near heat, surface shape error of the mirror, the interference intensity, and so on. Here, the relative position and orientation between the interferometer and

the piezostage is adjusted again till there exists less angular error between the optical axis and the measurement mirror. So, it can be evaluated that the performance of the interferometric calibration setup can be further improved when the setup is located in a well air-conditioned measurement box with additional heatproof and vibration isolation.

2 Calibration results for a piezostage

A pico-positioning stage (Nano-met3) with good positioning resolution in the picometer range, which will be used in PTB for nanoindentation with indentation depths down to a few picometers or large-range scanning probe microscopes, has been characterized using the proposed calibration setup. This stage has a displacement range of 5 μm in the z-axis direction, and has individually a displacement range of 75 μm in the x-axis/y-axis direction. For the purpose of quasi-static calibration of the direct current performance of this stage, three of the analog outputs (AOs) on the DAQ system are used to drive the stage with a user-programmable LabView software.

In the case of our calibration setup, the FPGA-based DAQ system has a resolution of 0.305 mV (V_{p-p}=20 V), yielding the resolution for displacement sensing with this approach to be about 170 pm. The displacements of the ultra-fine positioning stage are simultaneously measured using its built-in PicoQ® sensors and the interferometric calibration setup.

2.1 Linear calibration

After the stabilization of 24 h, the experiment is carried on in closed-loop mode of the piezostage and under nearly open-air condition (in plastic cover). The stage is driven in the forward and backward direction during the experiment. And the acquired data for the interferometer and the piezostage are filtered, and fitted linearly using least square estimate. Figure 5 shows the linear error within the full-scale range, and the maximum error is 0.61 nm. Then, the linearity is calculated approximately to be 1.2×10^{-4}.

To investigate the performance of the stage in open-

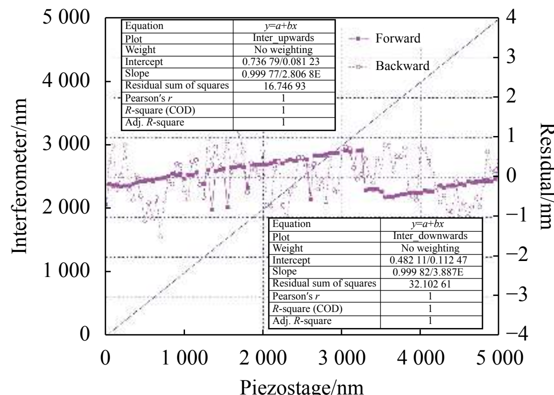

Fig.5 Interferometric calibration of a piezostage working in closed-loop mode

loop mode, another experiment is carried out under the same conditions. Due to the hysteresis effect of piezoestage, the data over the range of 1 000 nm are cut out of the full range and processed, as shown in Fig.6.

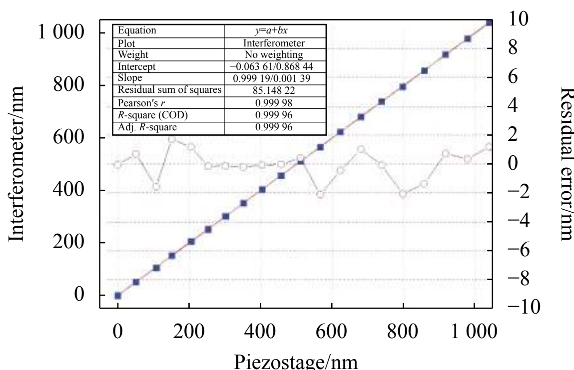

Fig.6 Interferometric calibration of a piezostage working in open-loop mode

It can be seen that the error variation is larger with the increasing displacement, and the stage under calibration has a variation of ±1.8 nm. According to the sensibility of the piezostage, it has an open-loop DC response of 639.4 pm/mV.

2.2 Resolution test

To assure the resolution of the nanostage under nearly open-air condition, a voltage output with 20 bit DAC is used to drive the nanostage. A 40 picometer amplitude pulse wave was performed using the 20 bit DAC in the user-programmable LabView software while the built-in sensor with a 24 bit ADC and the interferometer were respectively and simultaneously used to

measure the displacement of the nanostage. Figure 7 is the calibration result of the resolution of the nanostage using the proposed interferometric calibration setup.

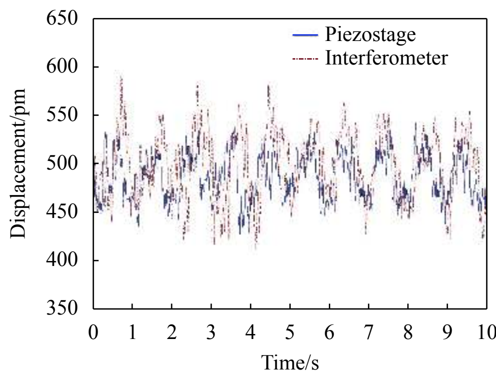

Fig.7 Closed-loop displacement of the piezostage measured by the integrated PicoQ® Sensor and the interferometer, respectively

Seen from Fig.7, the resolution of the piezostage can be calibrated with the NPL interferometer and can be up to at least 40 picometer. It indicates that the stage can provide a high-resolution driving displacement for MEMS technology.

2.3 Repeatability test

A pulse wave with the amplitude 2 000 nm was performed to drive the nanostage in the user's LabView software. The interval between the pulse signals was set to be 1 s. Then the initial position and the relative displacement of the calibrated piezostage were measured respectively using the interferometric setup and its built-in sensors. Figure 8 shows the interferometric calibration for repeatability of the piezostage at the modulated frequency of 400 Hz. It can be seen from Fig.8 that the initial

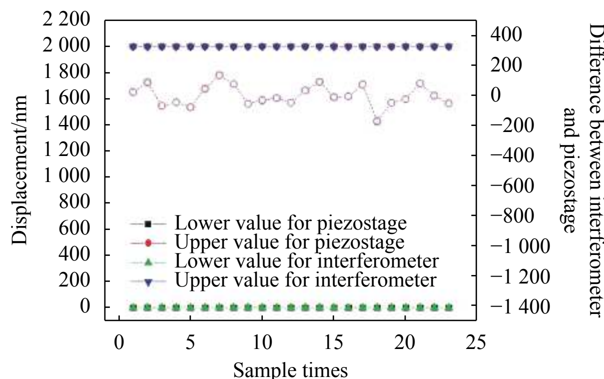

Fig.8 Interferometric calibration for repeatability of the piezostage

interferometric positioning error is less than 100 pm. So, the initial position is deemed to be identical. Computed the deviation of the amplitudes of the two signals, the displacement repeatability error is within 0.65 nm, and the standard deviation is above 0.2 nm. It indicates that the piezostage has a good repeatability and a strong stability in short time.

3 Conclusion

In this study, a traceable calibration methodology and system for the quantitative investigation of the quasi-static performance of ultra-fine positioning stage has been proposed and realized using the NPL differential plane mirror interferometer and the FPGA-based DAQ. In the case of quasi-static measurements, the interferometric displacement calibration setup under nearly open-air conditions has a resolution of 20 pm for a bandwidth of 1 Hz and a noise floor better than 10 pm/$\sqrt{\text{Hz}}$ for frequencies higher than 1 Hz. The assembling error of the measurement and reference mirrors was discussed and corrected successfully. The moving ultra-fine piezostage investigated quantitatively by the interferometric calibration system has an excellent performance of good linearity and strong repeatability under closed-loop mode. The further improvement of the sensitivity and nonlinearity of the interferometer, which can be possibly placed in a vacuum environment, is under consideration.

References:

[1] Dong Yanhao, Yang Hongbing, Zhang Lin, et al. Ultra-uniform nanocrystalline materials via two-step sintering [J]. *Advanced Functional Materials*, 2020, 31: 2007750.

[2] Hu Chunguang, Zha Ridong, Ling Qiuyu, et al. Super-resolution microscopy applications and development in living cell [J]. *Infrared and Laser Engineering*, 2017, 46(11): 1103002. (in Chinese)

[3] Du Chenhui, Gong Liang, Cai Xiaoyong, et al. Micro-nanometer scale vibration in imaging of metrological scanning electron microscope [J]. *Optics and Precision Engineering*, 2019, 27(4): 860-867. (in Chinese)

[4] Wu Ziruo, Cai Yanni, Wang Xingrui, et al. Investigation of

AFM tip characterization based on multilayer gratings [J]. ***Infrared and Laser Engineering***, 2020, 49(2): 0213001. (in Chinese)

[5] Shearer C J, Slattery A D, Stapleton A J, et al. Accurate thickness measurement of graphene [J]. ***Nanotechnology***, 2016, 27(12): 125704.

[6] Yacoot A, Koenders L, Wolff H. An atomic force microscope for the study of the effects of tip-sample interactions on dimensional metrology [J]. ***Meas Sci Technol***, 2007, 18(2): 350-359.

[7] Zhi Li, Uwe Brand, Helmut Wolff, et al. Broadband interferometric characterisation of nano-positioning stages with sub-10 pm resolution[C]//Proc SPIE, Optical Measurement Systems for Industrial Inspection X, 2017, 10329: 1032944.

[8] Podzorny Tomasz, Budzyń Grzegorz, Rzepka J. Linearization methods of laser interferometers for pico/nano positioning stages [J]. ***Optik-International Journal for Light and Electron Optics***, 2013, 124(23): 6345-6348.

[9] Wu C M, Su C S. Nonlinearity in measurements of length by optical interferometry [J]. ***Meas Sci Technol***, 1995, 7(1): 62-68.

[10] Yacoot A, Dows M. The use of X-ray interferometry to investigate the linearity of the NPL plane mirror differential optical interferometer [J]. ***Meas Sci Technolo***, 2000, 11(8): 1126-1130.

[11] Zeng Zhaoli, Zhang Shulian. Nanometrology technology in precision measurement [J]. ***Journal of Applied Optics***, 2012, 33(5): 846-854. (in Chinese)

[12] Zhu Minhao, Wu Xuejian, Wei Haoyun, et al. Closed-loop displacement control system for piezoelectric transducer based on optical frequency comb [J]. ***Acta Phys Sin***, 2013, 62(7): 070702. (in Chinese)

[13] Haroutunyan L A, Balyan M K. X-Ray on-axis Fresnel holography using three-block Fresnel zone plate interferometer [J]. ***Journal of Contemporary Physics (Armenian Academy of Sciences)***, 2020, 55(3): 248-253.

[14] Downs M J, Nunn J W. Verification of the sub-nanometric capability of an NPL differential plane mirror interferometer with a capacitance probe [J]. ***Meas Sci Technol***, 1998, 9(9): 1437-1440.

[15] Heydemann P L M. Determination and correction of quadrature fringe measurement errors in interferometers [J]. ***Appl Opt***, 1981, 20(19): 3382-3384.